$$PhN^{-}\cdot + CF_3CO_2CH_3 \not\rightarrow PhNCH_3 + CF_3CO_2^- \quad \Delta H^\circ = -54 \text{ kcal/mol}$$

$$\rightarrow PhNCOCF_3 + CH_3O\cdot \quad \Delta H^\circ = -14 \text{ kcal/mol} \qquad (4)$$

electron occupies an in-plane orbital on nitrogen.[1a] The acylation reactions are most easily rationalized with a mechanism in which the product-determining step is fragmentation of an intermediate formed by addition of $PhN^{-}\cdot$ to the carbonyl group (b, Figure 1, illustrated for reaction 1). This species is the radical anion of a 1,3-biradical and must be delocalized; however, as the negative charge is more stable on oxygen, we represent it in Figure 1 as an alkoxide. This process is thus the ionic analogue of an alkoxy radical fragmentation to an alkyl radical and a carbonyl compound. Formation of the chemically activated addition product in Figure 1 is estimated[6] to be 15 kcal/mol exothermic; this should be sufficient to overcome the barrier to decomposition to products. Alkoxy radical fragmentation barriers are typically[9] ~13 kcal/mol; we expect a lower barrier in this case due to the net exothermicity of the decomposition and the formation of the delocalized $PhNCHO$.

The mechanism in Figure 1 accounts for the observed products in reactions 1 and 4 but not in 2. Proton transfer in reaction 1 and S_N2 displacement in reaction 4 would each require 1,2-eliminations from the corresponding carbonyl addition products. The *A* factors for these processes are expected to be considerably lower than those for simple cleavage leading to the observed products; hence (assuming comparable activation energies) the reactions should proceed exclusively along the latter path. However, reaction 2 shows that proton transfer can dominate provided it is sufficiently exothermic. We now show that this observation is incompatible with a mechanism in which proton transfer in reaction 2 occurs via elimination from the carbonyl adduct.

Reaction with CH_3CH_2CHO produces only acylation while reaction with CH_3COCF_3 produces mainly proton transfer, although in the latter case acylation is still the most exothermic channel. While both product channels in reaction 2 are more exothermic than those in reaction 1, formation of the $PhN^{-}\cdot$ + CH_3COCF_3 addition product is also more exothermic than the corresponding addition to CH_3CH_2CHO. This is due to the biradical's electron affinity increase of[10] ~11 kcal/mol (estimated) arising from substitution of trifluoromethyl for ethyl. Thus, starting from the respective intermediates and assuming for the moment that proton transfer and acylation both proceed via these intermediates, ΔH°'s for the proton transfers in reactions 1 and 2 are approximately equal; the same holds for the acylations. The main difference between reactions 1 and 2 is therefore that the CH_3COCF_3 addition product is formed with more internal energy than is that with CH_3CH_2CHO. Quantum RRK calculations[11] show, however, that this extra activation will not cause the elimination (proton transfer) to dominate in the CH_3COCF_3 case, even with the assumption that elimination has a lower activation energy than cleavage. This is due to the *A* factor favoring the cleavage (acylation) pathway. Thus, this model, with branching occurring from the carbonyl adduct, cannot account for the different product distributions in reactions 1 and 2. We conclude that in these reactions proton transfer and acylation proceed via different pathways, with proton transfer becoming accessible only when it is strongly exothermic. The branching must thus occur before the carbonyl addition product is reached, presumably at *a*, the loose reactants complex. The product distribution is then governed by the relative energies of the transition states leading to proton transfer and carbonyl addition rather than by relative stabilities of the final products.

To our knowledge, these reactions have no counterpart in previous studies of gas-phase negative ion-molecule chemistry. We know of no other cases in which an anion displaces a free radical from a carbonyl center, although reactions involving nucleophilic attack on a carbonyl group are well-known.[12] However, there is a strong analogy with neutral free-radical chemistry. Alkyl radical displacements from carbonyl groups are common,[13] although reactions involving alkoxy radical displacement (analogous to reaction 4) seem to be unknown. It is currently accepted that these alkyl displacements involve alkoxy radical intermediates rather than direct displacements.[13]

We are currently continuing our investigations into the chemistry of $PhN^{-}\cdot$ as well as efforts to measure its photodetachment spectrum.

Acknowledgment. We are grateful to the National Science Foundation for support of this research and Dr. J. M. Jasinski for helpful discussions. We thank Professor R. N. McDonald for sharing his data with us prior to publication.

(6) ΔH°'s computed based on the following data: $\Delta H_f^\circ(PhN^{-}\cdot)$ = 60 kcal/mol;[1a] $\Delta H_f^\circ(PhNCOCF_3)$ = −196.5 kcal/mol, based on group additivity[7] and estimated $\Delta H^\circ_{acid}(PhNHCOCF_3)$ = 338 kcal/mol; $\Delta H_f^\circ(PhNCHO)$ = −29.4 kcal/mol, based on estimated $\Delta H^\circ_{acid}(PhNHCHO)$ = 351 kcal/mol; $\Delta H_f^\circ(PhNCOCH_2CH_3)$ = −47 kcal/mol, based on estimated ΔH°_{acid}-$(PhNHCOCH_2CH_3)$ = 352 kcal/mol; ΔH_f°(b, Figure 1) = 0 kcal/mol, assuming $EA(PhN\text{-}CH(O\cdot)CH_2CH_3)$ = 50 kcal/mol (EA = electron affinity). All other ΔH_f°'s are taken from ref 4, 7, and 8.

(7) Benson, S. W. "Thermochemical Kinetics", 2nd ed.; Wiley-Interscience: New York, 1976.

(8) O'Neal, H. E.; Benson, S. W. *Free Radicals* **1973**, *2*, Chapter 17.

(9) Kochi, J. K. *Free Radicals*, **1973**, *2*, Chapter 23.

(10) Based on calculated electron affinities of $OCH_2CH_2CH_3$ and OCH_2CF_3 using bond strength and gas-phase acidity data from ref 4.

(11) Robinson, P. J.; Holbrook, K. A. "Unimolecular Reactions"; Wiley-Interscience: New York, 1972; Chapter 3.

(12) (a) Asubiojo, O. I.; Brauman, J. I. *J. Am. Chem. Soc.* **1979**, *101*, 3715. (b) Bowie, J. H. *Acc. Chem. Res.* **1980**, *13*, 76.

(13) See, for instance: Ingold, K. U; Roberts, B. P. "Free-Radical Substitution Reactions"; Wiley-Interscience: New York, 1971; p 86 ff and references cited therein.

Internal Rotation in Liquid 1,2-Dichloroethane and *n*-Butane[1]

William L. Jorgensen†

Department of Chemistry, Purdue University
West Lafayette, Indiana 47907

Received July 14, 1980

Solvent effects on the conformational preferences of 1,2-dihaloethanes have been extensively analyzed with diffraction and spectroscopic techniques.[2] The increased gauche/trans ratios observed in polar solvents have been explained traditionally by simple electrostatics; the gauche rotamers have large dipole moments which lead to dipole–dipole stabilization in condensed phases.[2] The ability to perform meaningful theoretical studies of such conformational problems in liquids appears to be possible by using molecular dynamics[3] and Monte Carlo statistical mechanics calculations.[4] However, to date, the theoretical work has not modeled a system for which experimental conformational data are available. Consequently, a Monte Carlo simulation of liquid 1,2-dichloroethane (DCE) has been carried out. The results presented here confirm that this method can reproduce the observed solvent shifts. In addition, pure liquid *n*-butane has been modeled for comparison and to reinvestigate the predicted condensed phase effect on the conformational equilibrium for this important prototype system.[3,5]

† Camille and Henry Dreyfus Foundation Teacher-Scholar, 1978–1983; Alfred P. Sloan Foundation Fellow, 1979–1981.

(1) Quantum and Statistical Mechanical Studies of Liquids. 15. Work supported by the National Science Foundation (CHE78-19446).

(2) For a review, see: Abraham, R. J.; Bretschneider, E. In "Internal Rotation in Molecules"; Orville-Thomas, W. J., Ed.; Wiley: London, 1974; Chapter 13.

(3) (a) Ryckaert, J. -P.; Bellemans, A. *Discuss. Faraday Soc.* **1978**, *66*, 95. (b) Weber, T. A. *J. Chem. Phys.* **1978**, *69*, 2347. (c) Rebertus, D. W.; Berne, B. J.; Chandler, D. *Ibid.* **1979**, *70*, 3395.

(4) Jorgensen, W. L. *J. Am. Chem. Soc.* **1981**, *103*, 335, 341, 345.

0002-7863/81/1503-677$01.00/0

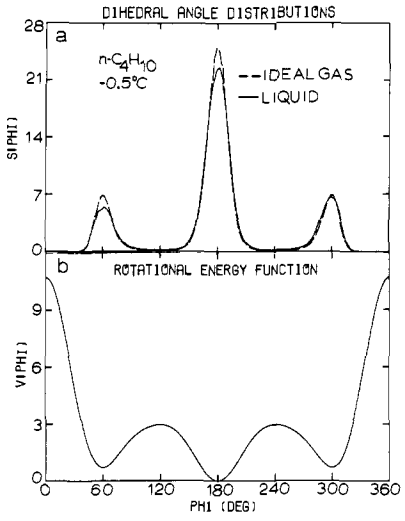

Figure 1. (a) Computed population distributions for the dihedral angle about the central CC bond in *n*-butane. Units for $S(\phi)$ are (mole fraction/deg) $\times 10^{-3}$. (b) Potential function (kcal/mol) for rotation about the central CC bond in *n*-butane.

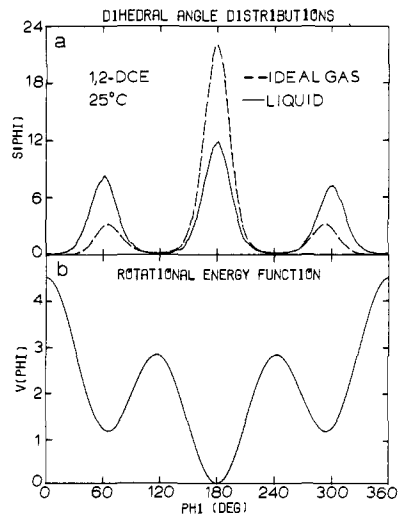

Figure 2. (a) Computed population distributions for the dihedral angle about the CC bond in DCE. (b) Potential function (eq 2) for rotation about the CC bond in DCE. Units are the same as in Figure 1.

The Monte Carlo calculations were executed in the NVT ensemble by using standard procedures including cubic samples of 128 monomers, periodic boundary conditions, Metropolis sampling, and spherical cutoffs at 11 Å for the intermolecular potentials.[4] The simulations were run at 25 °C for DCE and at the boiling point (–0.5 °C) for butane. The volume of the periodic cubes was determined from the corresponding experimental densities for liquid DCE (1.2457 g cm^{-3}) and *n*-butane (0.602 g cm^{-3}).[6] The intermolecular interactions were represented in the TIPS format.[4] Each monomer contains four interaction sites, the chlorines and methylenes for DCE and the methyl and methylene groups for *n*-butane, which interact intermolecularly via Coulomb and Lennard-Jones terms (eq 1).[4] The A and C parameters for methyl

$$\Delta E = \sum_{i}^{\text{on } A} \sum_{j}^{\text{on } B} \left(\frac{q_i q_j e^2}{r_{ij}} + \frac{A_i A_j}{r_{ij}^{12}} - \frac{C_i C_i}{r_{ij}^{6}} \right) \quad (1)$$

and methylene groups were reported previously and the sites in *n*-butane are neutral ($q = 0$).[4] The parameters for chlorine were chosen to yield reasonable (1) liquid-phase dipole moments for alkyl chlorides and (2) gas-phase geometries and dimerization energies for HCl and Cl_2 dimers in comparison with results of ab initio quantum mechanical calculations.[7] The resultant A, C, and q for chlorine are 2449 (kcal Å^{12}/mol)$^{1/2}$, 51 (kcal Å^6/mol)$^{1/2}$, and –0.25 e. To preserve neutrality, q for the methylene group in DCE is then +0.25. Standard geometries were used for the monomers that are consistent with diffraction data for the gases: r(CC) = 1.530 Å, r(CCl) = 1.785 Å, and ∠CCC = ∠CCCl = 109.47°.[4,8] The last components are the potential functions, $V(\phi)$, for internal rotation about the central CC bonds in the monomers. For *n*-butane, the revised Scott-Scheraga potential was adopted.[3a] For DCE, a function given by eq 2 was derived that fits the available gas-phase experimental data.[8-10] The

$$V(\phi) = {}^1/_2V_1(1 + \cos\phi) + {}^1/_2V_2(1 - \cos 2\phi) + {}^1/_2V_3(1 + \cos 3\phi) \quad (2)$$

resultant V_1, V_2, and V_3 are 1.933, -0.333, and 2.567 kcal/mol. The functions are illustrated in Figures 1b and 2b. The gauche minima are 1.14 kcal/mol above trans for DCE and 0.70 kcal/mol for *n*-butane, while the trans to gauche barrier heights are 2.81 and 2.95 kcal/mol, respectively.

In the Monte Carlo calculations, new configurations were generated by randomly picking a monomer, translating it in all three Cartesian directions, rotating it about one axis, and performing the internal rotation. Acceptance rates of 40–50% were obtained by using ranges of *ca.* ±0.15 Å and ±15° for the translations and angular variations. Equilibration was carefully established for *n*-butane; two runs were made with the monomers initially all cis and initially all trans. The two calculations required 800K configurations each to converge to the same total and internal energies and gauche/trans ratio. Final averaging occurred for one run over an additional 700K configurations. The initial configuration for DCE was derived from one in the simulation of *n*-butane. Equilibration was completed in 700K configurations and final averaging was performed over an additional 405K. Monitoring the barrier crossings during the averaging also confirmed the equilibration in both cases. There were nearly equal numbers of barrier crossings in each direction; e.g., for DCE there were 194 gauche to trans, 193 trans to gauche, 81 gauche$^+$ to gauche$^-$, and 79 gauche$^-$ to gauche$^+$ crossings during the last 405K. Gauche to gauche crossings did not occur for liquid *n*-butane due to the much higher barrier. The total number of barrier crossings in the final 700K for *n*-butane was *ca.* 850; however, only about 1 in 5 *crossings* yields a true *transition* such that the monomer stays in the new well for an extended period.

The computed heats of vaporization obtained as usual[4] including cutoff corrections of *ca.* 0.3 kcal/mol are 8.40 ±0.02 kcal/mol for DCE at 25 °C and 5.39 ±0.02 kcal/mol for *n*-butane at –0.5 °C, which are in excellent agreement with the experimental values of 8.40 and 5.35 kcal/mol.[11,12] The computed radial distribution functions (RDF's) for the liquids are generally similar with broad, low peaks, though the peaks for DCE are somewhat sharper. Integration yields coordination numbers of 12–14. Analysis of stereo plots of configurations reveals a tendency to maximize CH_2···Cl interactions in DCE. This is supported by the shift and sharpening of the first peak for the CH_2···CH_3 RDF in *n*-butane at 5.1 Å to the peak at 4.0 Å for CH_2···Cl in DCE. Full thermodynamic and structural details will be presented elsewhere.[7] However, it is noted that an NPT simulation has been carried out for liquid *n*-butane at 1 atm.[13] The computed density of 0.618 g cm^{-3} is within 3% of the experimental value which further

(5) Pratt, L. R.; Hsu, C. S.; Chandler, D. *J. Chem. Phys.* **1978**, *68*, 4202.
(6) (a) Wilhelm, E.; Schano, R.; Becker, G.; Findenegg, G. H.; Kohler, F. *Trans. Faraday Soc.* **1969**, *65*, 1443. (b) Rossini, F. D.; Pitzer, K. S.; Arnett, R. L.; Brown, R. M.; Pimentel, G. C. "Selected Values of Physical and Thermodynamic Properties of Hydrocarbons and Related Compounds"; American Petroleum Institute; Carnegie Press: Pittsburgh, 1953.
(7) Complete details will be provided in a full paper: Jorgensen, W. L.; Bigot, B.; Binning, R. C. *J. Am. Chem. Soc.*, in press.
(8) Kveseth, A. *Acta Chem. Scand. Ser. A* **1975**, *A29*, 307.
(9) Lowe, J. P. *Prog. Phys. Org. Chem.* **1968**, *6*, 1.
(10) Tanabe, K. *Spectrochim. Acta* **1972**, *28A*, 407.
(11) (a) Wadso, I. *Acta Chem. Scand.* **1968**, *22*, 2438. (b) Aston, J. G.; Messerly, G. H. *J. Am. Chem. Soc.* **1940**, *62*, 1917.
(12) The computed standard deviations reported here (2σ) were obtained from averages for each increment of 15–20K configurations.
(13) Jorgensen, W. L. *J. Am. Chem. Soc.*, to be submitted.

supports the choice of the TIPS parameters for alkyl groups.

The computed distribution functions, $S(\phi)$, for the dihedral angle in the liquids are compared to the ideal gas results in Figures 1a and 2a. The increased gauche population in liquid DCE is dramatic, while the condensed phase effect for liquid *n*-butane is negligible. The dominance of the electrostatics and not the lower molar volume in producing the shift for DCE was proven by a Monte Carlo simulation with the Coulomb terms deleted.[7] When the charges are set to zero for DCE and all other parameters and conditions are unchanged, the computed $S(\phi)$ is nearly identical with the ideal gas result.[7] The trans populations are obtained by integrating $S(\phi)$ from 120 to 240°, the remainder being gauche. For DCE, the computed trans populations are 76.5% for the ideal gas and (43.5 ± 0.5)% for the liquid which agree well with the estimates from IR data of (77 ± 2)% and (35 ± 4)% at 25 °C.[10] For *n*-butane, the computed trans populations are 67.7% for the ideal gas and (67.1 ± 0.8)% for the liquid. The NPT simulation at 1 atm is in accord predicting (67.8 ± 1.3)% trans for liquid *n*-butane at −0.5 °C.[13] Thus, no statistically significant condensed phase effect on the conformational equilibrium for liquid *n*-butane at the standard density is revealed. This agrees with Flory's traditional position on polymer melts;[14] however, it contrasts some earlier, less extensive theoretical results which were interpreted as indicating a "significant" shift toward increased gauche population in the pure liquid.[3a,5] Finally, it is noted that correcting for the rigid constraints on the bond lengths and bond angles in a recent molecular dynamics simulation of *n*-butane in CCl_4 did not alter the computed gauche/trans ratio.[15]

(14) Flory, P. J. "Statistical Mechanics of Chain Molecules"; Wiley-Interscience: New York, 1969; p 57.
(15) Chandler, D.; Berne, B. J. *J. Chem. Phys.* **1979**, *71*, 5386.

Design, Synthesis and Characterization of a Cytotoxic Peptide with Melittin-Like Activity

William F. DeGrado, F. J. Kézdy,* and E. T. Kaiser*

Departments of Chemistry and Biochemistry
The University of Chicago
Chicago, Illinois 60637
Received September 18, 1980

Recently, we have been testing the hypothesis that the binding characteristics of certain proteins, such as those of apolipoproteins to interfaces, are determined by an important secondary structural feature, the amphiphilic α helix.[1-3] We have shown that a model docosapeptide, with minimum homology to apolipoprotein A-I (apo A-I), has the binding chracteristics of apo A-I by criteria of its binding to phospholipid single bilayer vesicles, surface activity, and ability to activate lecithin:cholesterol acyltransferase.[4,5] The main toxic component from bee venom, melittin[6] (Figure 1A) is a hexacosapeptide which has many properties in common with the apolipoproteins. It binds to phospholipid bilayers,[7-14] forms stable monolayers at the air-water interface,[7] and is capable of forming an α helix upon tetramerization or when bound to sodium dodecyl sulfate micelles or phospholipid bilayers.[13,14] This suggested to us that the amphiphilic α helix might be essential for the biological activity of melittin but only to the extent that it is providing a secondary structure. A second feature which appears to be necessary for the biological activity of melittin is the highly basic C-terminal hexapeptide, since synthetic melittin (1-20),[15] which lacks this hexapeptide, is as surface active as melittin but is not biologically active as measured by the erythrocyte lysis assay. In addition, the length of the amphiphilic helical segment appears important since segments with shortened N-terminal sequences such as melittin (8-26) are also very poor lytic agents.[14] Thus, the essential requirements for a lytic agent such as melittin appear to be an eicosapeptide segment capable of forming an amphiphilic α helix, followed by a highly basic C-terminal hexapeptide which is recognized by the cell. To test this hypothesis, we have synthesized peptide **1** (Figure 1A) which is homologous to melittin only in the C-terminal hexapeptide region. Peptide **1** has a higher potential to form amphiphilic α helices than melittin, and we will show that it epitomizes many of the biological and physical properties of melittin.

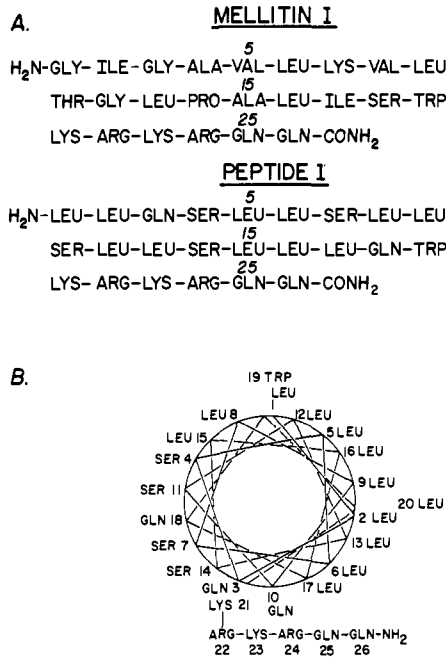

Figure 1. (A) Amino acid sequences of melittin I and peptide **1**. (B) Axial projection of the α-helical region of peptide **1** showing the relative location of the side chains with the segregation of the hydrophobic and hydrophilic residues.

As illustrated by the helical projection in Figure 1B, residues 1-20 of **1** have been chosen to form an amphiphilic helix with minimum homology to melittin while maintaining a hydrophobic-hydrophilic balance related to the two amphiphilic α helical segments of melittin (2-13) and (15-21). The hydrophobic side of the helix was composed of Leu residues, chosen for reason of their high helix-forming potential,[16] hydrophobicity, and electrical neutrality. While Gln seemed an ideal choice for the neutral hydrophilic residues, some Ser residues were included to increase the hydrophilicity of the model, allowing us to match the amphiphilicity of the native peptide. A Trp residue was left at position 19 for future studies of intrinsic fluorescence, and the C-terminal hexapeptide of melittin was retained as such.

Peptide **1** was synthesized by the solid-phase method on 1% cross-linked divinylbenzene–polystyrene by using the symmetric

(1) Segrest, J. P.; Jackson, R. L.; Morrisett, J. P.; Gotto, A. M., Jr. *FEBS Lett.* **1974**, *38*, 247.
(2) Morrisett, J. D.; Jackson, R. L.; Gotto, A. M., Jr. *Biochim. Biophys. Acta* **1977**, *472*, 93.
(3) Fukushima, D.; Kaiser, E. T.; Kézdy, F. J.; Kroon, D. J.; Kupferberg, J. P.; Yokoyama, S. *Ann. N.Y. Acad. Sci.* **1980**, *348*, 365.
(4) Fukushima, D.; Kupferberg, J. P.; Yokoyama, S.; Kroon, D. J.; Kaiser, E. T.; Kézdy, F. J. *J. Am. Chem. Soc.* **1979**, *101*, 3703.
(5) Yokoyama, S.; Fukushima, D.; Kézdy, F. J.; Kaiser, E. T. *J. Biol. Chem.* **1980**, *255*, 7333.
(6) Habermann, E. *Science (Washington, DC)* **1972**, *177*, 314.
(7) Sessa, G.; Freer, J. H.; Colacicco, G.; Weissmann, G. *J. Biol. Chem.* **1969**, *244*, 3575.
(8) Mollay, C.; Kreil, G. *Biochim. Biophys. Acta* **1973**, *316*, 196.
(9) Verma, S. P.; Wallach, D. F. H.; Smith, I. C. P. *Biochim. Biophys. Acta* **1974**, *345*, 129.
(10) Mollay, C. *FEBS Lett.* **1976**, *64*, 65.
(11) Dufourcq, J.; Faucon, J. F. *Biochim. Biophys. Acta* **1977**, *467*, 1.
(12) Galla, H. J.; Hartmann, W.; Sackmann, E. *Ber. Bunsenges, Phys. Chem.* **1978**, *82*, 917.
(13) Drake, A. F.; Hider, R. C. *Biochim. Biophys. Acta* **1979**, *555*, 371.
(14) Dawson, C. R.; Drake, A. F.; Helliwell, J.; Hider, R. C. *Biochim. Biophys. Acta*, **1978**, *510*, 75.
(15) Schröder, E.; Lübke, K.; Lehmann, M.; Beetz, I. *Experientia* **1971**, *27*, 764.
(16) Chou, P. Y.; Fasman, G. D. *Annu. Rev. Biochem.* **1978**, *47*, 251.

0002-7863/81/1503-679$01.00/0